

Coherent backscattering in the Fock space of ultracold bosonic atoms

Peter Schlagheck¹ and Julien Dujardin¹

¹*Département de Physique, University of Liege, 4000 Liège, Belgium*

We present numerical evidence for the occurrence of coherent backscattering in the Fock space of a small disordered Bose-Hubbard system consisting of four sites and containing five particles. This many-body interference phenomenon can most conveniently be seen in time evolution processes that start from a Fock state of the Bose-Hubbard system. It manifests itself in an enhanced detection probability of this initial state as compared to other Fock states with comparable total energy. We argue that coherent backscattering in Fock space can be experimentally measured with ultracold bosonic atoms in optical lattices using state-of-the-art single-site detection techniques. A synthetic gauge field can be induced in order to break time-reversal symmetry within the lattice and thereby destroy coherent backscattering. While this many-body interference effect is most prominently visible in the presence of eigenstate thermalization, we briefly discuss its significance in the opposite regime of many-body localization.

I. INTRODUCTION

The eigenstate thermalization hypothesis can be considered to be a fundamental cornerstone of quantum statistical physics [1–3]. It basically assumes for a quantum many-body system that its eigenstates are equidistributed in phase space along the energy shell associated with the corresponding eigenvalue (provided the total energy is the only constant of motion of the system [4]). As a consequence, the time average of an observable that is evaluated along the evolution of a many-body wave packet of this system can be determined from the phase-space average of this observable along the energy shells that are covered by this wave packet [3], which is referred to as ergodicity.

While the eigenstate thermalization hypothesis can safely be taken for granted in dilute and weakly interacting three-dimensional quantum gases, it is challenged and ultimately invalidated e.g. in strongly disordered one-dimensional many-body systems due to the occurrence of many-body localization [5–14]. The latter can, in this particular context, be understood as a generalization of Anderson localization [15] to the many-body domain. Indeed, all single-particle eigenmodes of an infinite one-dimensional disordered system can be shown to be spatially localized even for weak disorder [15], and the presence of a moderate two-body interaction may not be sufficient to efficiently couple spatially distant eigenmodes with each other. In that case, a many-body wave packet cannot explore the entire energy shell and will remain localized in the vicinity of the phase space region in which it was initially prepared.

The present contribution is concerned with a less spectacular and more subtle localization phenomenon. It arises in the regime of eigenstate thermalization, where we should expect ergodicity to occur, and can be seen as the extension of the concept of *weak localization* to the many-body domain. From a semiclassical point of view, weak localization is essentially caused by the constructive interference between backscattered classical paths of the system and their time-reversed counterparts. This latter

phenomenon of coherent backscattering was experimentally observed in a number of physical contexts, ranging from laser light scattering off disordered media [16, 17] to, more recently, atomic Bose-Einstein condensates moving in optical speckle fields [18]. It implies a slight enhancement of the reflection and, in turn, also a slight reduction of the transmission probability [19] in disordered or chaotic wave scattering configurations.

Translated to the many-body domain, coherent backscattering gives rise to a slight but significant deviation from quantum ergodicity, since the initial state of a many-body wave packet thereby has an enhanced probability to be encountered during the time evolution of this wave packet than any other many-body state on the same energy shell. This many-body coherent backscattering phenomenon was promoted and discussed in detail in Refs. [20–23] considering both bosonic [20, 21] and fermionic systems [22, 23]. In Ref. [20], in particular, it was argued and confirmed through numerical simulations that a disordered many-body Bose-Hubbard system which is initially prepared in one of its Fock states will, in the course of time evolution, be encountered and detected about twice as often in this initial state as compared to any other Fock state with comparable total energy.

The main purpose of this paper is to investigate this delicate but robust many-body interference phenomenon within a relatively small system that can possibly be realized in an experiment using ultracold bosonic quantum gases. We specifically consider for this purpose a disordered Bose-Hubbard ring containing four sites, which describes a single plaquette of a two-dimensional optical square lattice exhibiting random on-site energies. This Bose-Hubbard ring is supposed to be loaded with five particles. As we shall show below, the effect of coherent backscattering in Fock space can indeed be encountered in such a microscopic many-body system, and its observation with ultracold bosonic atoms is within the reach of present-day state-of-the-art experiments.

A proposal for the experimental protocol that can be implemented for this purpose is outlined and discussed in Section II. Section III discusses the evolution of coherent backscattering in Fock space as a function of time as well

as its dephasing in the presence of an artificial gauge field that induces complex inter-site hopping matrix elements within the Bose-Hubbard ring and thereby breaks time-reversal invariance. In Section IV we describe how to define and numerically compute classical predictions for the average detection probabilities of Fock states, using the van Vleck–Gutzwiller propagator and the diagonal approximation. Finally, Section V discusses to which extent coherent backscattering in Fock space plays a role also in the regime of many-body localization.

II. THE PROPOSED EXPERIMENTAL PROCEDURE

We consider a finite number of ultracold bosonic atoms that are confined within a single plaquette of a two-dimensional optical lattice. This plaquette can be isolated from the rest of the lattice by means of a red-detuned laser beam that is perpendicularly focused on the lattice or by generating a two-dimensional superlattice, in close analogy with Refs. [24, 25]. This latter approach would yield a periodic checkerboard arrangement of plaquettes within which near-identical experiments can be performed in parallel.

Within the single-band approximation, the many-body dynamics of this configuration can be described by the Bose-Hubbard Hamiltonian

$$\hat{H} = \sum_{l=1}^L \left[\epsilon_l \hat{b}_l^\dagger \hat{b}_l - J \left(e^{i\varphi} \hat{b}_l^\dagger \hat{b}_{l-1} + e^{-i\varphi} \hat{b}_{l-1}^\dagger \hat{b}_l \right) + \frac{U}{2} \hat{b}_l^\dagger \hat{b}_l^\dagger \hat{b}_l \hat{b}_l \right] \quad (1)$$

with $L = 4$, where \hat{b}_l^\dagger and \hat{b}_l respectively represent the bosonic creation and annihilation operators associated with the site l (we formally identify $\hat{b}_0 \equiv \hat{b}_L$, $\hat{b}_0^\dagger \equiv \hat{b}_L^\dagger$). ϵ_l denotes the on-site energy of the site $l = 1, \dots, L$, U represents the on-site interaction energy between two atoms, and J is the hopping amplitude between adjacent sites. Time-reversal symmetry can be broken by imposing a finite hopping phase $\varphi \neq 0$ which can be engineered through the application of a synthetic gauge field [26–28].

The plaquette is to be loaded with a finite number of atoms in the deep Mott insulator regime where inter-site hopping can be neglected. This loading process is supposed to take place in such a way that a well-defined single Fock state in the site basis is reliably obtained as initial state of this many-body system for a suitable choice of the on-site energies ϵ_l [29]. For the sake of definiteness, we consider the initial state $|\mathbf{n}^{(i)}\rangle \equiv |n_1^{(i)}, n_2^{(i)}, n_3^{(i)}, n_4^{(i)}\rangle = |1, 2, 2, 0\rangle$ in the following, where n_l denotes the number of atoms located on the site l .

At time $t = 0$ inter-site hopping is switched on, such that the atoms can move from site to site. We furthermore suppose that the on-site energies of the individual sites acquire random values at $t = 0$, which in practice can be achieved by means of an optical speckle field

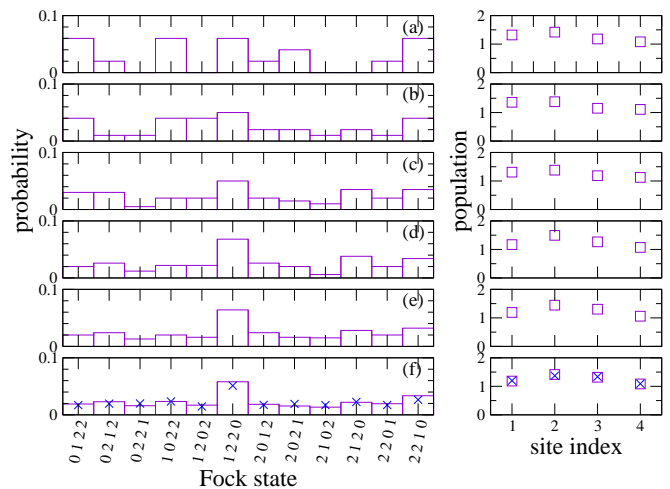


Figure 1: Numerical simulation of a measurement process. Plotted are, in the left column, the probabilities for detecting a given Fock state and, in the right column, the average populations on each site of the lattice. These data are determined from the accumulated measurement outcomes that are obtained after (a) 50, (b) 100 (c) 200, (d) 500, (e) 1000, and (f) 2000 repetitions of the numerical experiment. The blue crosses in (f) show the average quantum probabilities (left) and populations (right) obtained from the numerical integrations of the time evolution generated by the Bose-Hubbard Hamiltonian (1). The calculation was done for the initial state $|1, 2, 2, 0\rangle$, the lattice parameters $U = J$, $\varphi = 0$, $W = 4J$, and the evolution time $T = 10\hbar/J$. Only Fock states that have the same interaction energy as the initial state are shown in the left column.

[30, 31]. For the sake of numerical convenience, we assume for the following that for $t > 0$ the on-site energies are given by uncorrelated random values $\epsilon_l \in [0, W]$ that result from a uniform probability distribution characterized by the energy scale W [32].

The inter-site hopping is to be switched off at a given final time $T > 0$, such that the sites are again isolated. Subsequently, the populations of the individual sites of the lattice have to be detected site by site, yielding a result that can be represented by the final Fock state $|\mathbf{n}\rangle \equiv |n_1, n_2, n_3, n_4\rangle$. From the experimental point of view, this latter task appears to represent the most challenging part of this proposal. It could possibly be achieved by combining the high-resolution imaging techniques pioneered in Refs. [33, 34], which allow to detect binary populations (i.e., $n_l = 0$ or 1) of individual lattice sites, with a free expansion of the atoms onto previously unpopulated sites of the two-dimensional optical lattice, in close analogy with Ref. [35].

The idea is now to repeat this particular experiment many times, each time starting with the preparation of the same initial state $|\mathbf{n}^{(i)}\rangle$, in order to measure the probabilities for obtaining a given final state $|\mathbf{n}\rangle$ with sufficient statistical accuracy. A disorder average is to be introduced by randomly varying the on-site energies ϵ_l from one experiment to the next one.

Figure 1 shows a numerical simulation of the outcome resulting from such a sequence of experiments, for the parameters $U = J$, $W = 4J$, $\varphi = 0$, and for the final time $T = 10\hbar/J$. This simulation is performed by means of numerical integrations of the time evolution generated by the Bose-Hubbard Hamiltonian (1) [36], each one being carried out for a given random choice of on-site energies. The resulting quantum probabilities $p_{\mathbf{n}}$ for obtaining a particular final state $|\mathbf{n}\rangle$ are then used to simulate a measurement process corresponding to a projection onto one of those Fock states.

We see that some 1000 repetitions of this experiment would be necessary in order to achieve statistical convergence. At that point, all Fock states $|\mathbf{n}\rangle \neq |\mathbf{n}^{(i)}\rangle$ that exhibit the same interaction energy as the initial state $|\mathbf{n}^{(i)}\rangle = |1, 2, 2, 0\rangle$ are detected with about equal probability, which indicates that we are in a regime of eigenstate thermalization. There is one exception, however: the initial state $|\mathbf{n}^{(i)}\rangle$ is significantly more often detected than those other Fock states.

This notable deviation from quantum ergodicity in Fock space seems to have a tiny but significant impact onto the average populations per site, as can be seen in the right column of Fig. 1. While the naive application of the ergodic hypothesis would straightforwardly yield a uniform average distribution of atoms within the plaquette, the populations on the sites $l = 2$ and 3 are found to be enhanced by about 20 percent as compared to the sites $l = 4$ and $l = 1$, respectively, which is consistent with the initial state $|1, 2, 2, 0\rangle$. Obviously, much less repetitions of the experiment are required in order to obtain a satisfactory statistical convergence of the average populations per site as compared to the probabilities in Fock space. We note that those average populations can be measured with a simpler experimental scheme than the one that we outline above, namely by performing many near-identical experiments in parallel within a two-dimensional superlattice configuration, and by generalizing the Brillouin zone mapping technique used in Refs. [24, 25] to two spatial dimensions, such that the populations of the sites can be clearly distinguished in momentum space after a free expansion of the atomic cloud.

III. COHERENT BACKSCATTERING IN FOCK SPACE

To confirm that this signature of non-ergodicity is not a transient phenomenon that would disappear after longer evolution times, we show in Fig. 2 snapshots of the time evolution of the probabilities for detecting a given Fock state, for the same initial state $|1, 2, 2, 0\rangle$ and the same lattice parameters $U = J$, $W = 4J$ as in Fig. 1. We clearly see that after an initial transient regime, which is very specific to the initial state under consideration and which lasts about one hopping period $\tau = 2\pi/J$, a stable and practically stationary probability distribution is obtained in the Fock space. As in Fig. 2, the initial state is

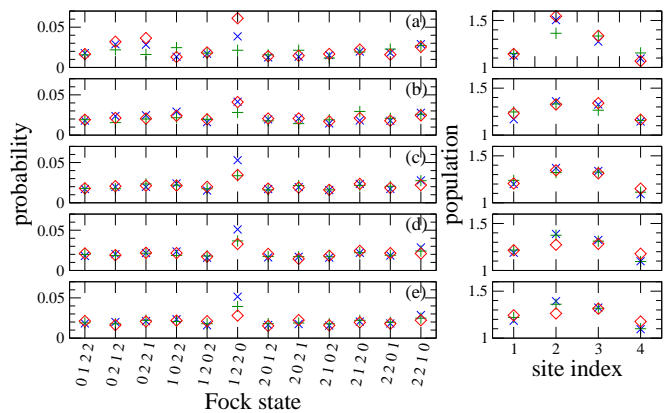


Figure 2: Time evolution of the probabilities for detecting a given Fock state (left column) and of the average populations per site (right column), shown for $Jt/\hbar = 2$ (a), 5 (b), 10 (c), 20 (d), and 50 (e). The quantum calculations were done for the initial state $|1, 2, 2, 0\rangle$, the lattice parameters $U = J$, $W = 4J$, and the hopping phases $\varphi = 0$ (blue \times) as well as $\varphi = 0.1\pi$ (green $+$). Red diamonds show the corresponding classical predictions for $\varphi = 0$.

characterized by a significant enhancement of its detection probability as compared to other Fock states with comparable interaction energy, the latter being detected with equal probability.

The origin of this enhancement can, to a dominant extent, be attributed to coherent backscattering in Fock space. This latter phenomenon generally refers to an enhanced probability for backscattering of a wave that propagates in the presence of chaos or disorder, owing to the systematic and robust constructive interference between backscattered paths and their time-reversed counterparts [37]. It is at the origin of weak localization in mesoscopic electronic conduction process [37] and was recently observed with ultracold bosonic matter waves [18, 38]. As was explained in Ref. [20], the generalization of the concept of coherent backscattering to a many-body Bose-Hubbard lattice can be done by considering each site of the lattice as being an independent oscillator-like degree of freedom. Classical “paths” within such a lattice correspond then to solutions of a discrete Gross-Pitaevskii equation, as we shall further elaborate in the subsequent section. Backscattered paths start out with a given set of amplitudes per site (namely the ones that correspond to the initial state $|\mathbf{n}^{(i)}\rangle$) and end up with exactly the same amplitudes, while associated phases may be arbitrary.

A characteristic signature of coherent backscattering and weak localization is its sensitivity to any breaking of time-reversal invariance induced by means of a weak gauge field (which in the electronic case would most naturally be given by a magnetic field). While such a gauge field may not necessarily modify the classical paths in an appreciable manner, it does affect the associated phases in such a way that the interference between a backscattered path and its time-reversed counterpart is

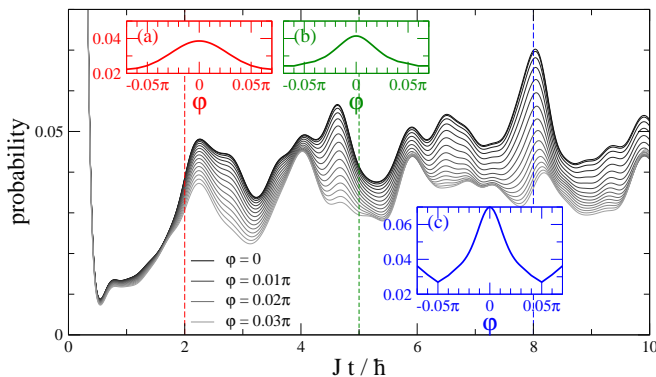


Figure 3: Time evolution of the probability to detect the initial state $|1, 2, 2, 0\rangle$ plotted for the hopping phases $\varphi = 0$ (darkest curve), $0.002, 0.004, \dots, 0.03$ (lightest curve) at the lattice parameters $U = J, W = 4J$. The insets show these probabilities as a function of the hopping phase φ at fixed times $t = 2\hbar/J$ (left inset, shown in red), $t = 5\hbar/J$ (middle inset, shown in green), and $t = 8\hbar/J$ (right inset, shown in blue).

no longer entirely constructive. As a consequence, the coherent backscattering amplitude generally decreases with increasing strength of the gauge field.

This dephasing behaviour is indeed found in our four-sites Bose-Hubbard ring. As can be seen in Fig. 2, the presence of a weak hopping phase $\varphi = 0.1\pi$ significantly reduces the probability for detecting the initial state as compared to the time-reversal invariant case $\varphi = 0$, whereas the probabilities for detecting other Fock states $|\mathbf{n}\rangle \neq |\mathbf{n}^{(i)}\rangle$ are not appreciably modified. Figure 3 shows the probability to detect the initial state as a function of time for various hopping phases. We see in the insets that the backscattering probability continuously decreases with increasing hopping phase for $|\varphi| \lesssim 0.05\pi$, which is a clear signature of weak localization.

IV. COMPARISON WITH CLASSICAL PREDICTIONS

To ultimately confirm that the enhancement of the detection probability of the initial state as compared to other Fock states with comparable total energy arises due to a quantum interference phenomenon taking place in the Fock space of the bosonic many-body system, we compare the numerically computed detection probabilities for the final state $|\mathbf{n}\rangle \equiv |n_1, \dots, n_L\rangle$ with classical predictions that precisely neglect the presence of those many-body interferences. To this end, we employ the framework of the semiclassical van Vleck–Gutzwiller propagator [39]. The latter allows one to express the matrix elements of the time evolution operator of the bosonic many-body system in its Fock basis as a sum over classical trajectories that evolve according to the

discrete nonlinear Schrödinger equation

$$i\hbar \frac{d}{dt} \psi_l(t) = \epsilon_l \psi_l(t) - J [\psi_{l+1}(t) + \psi_{l-1}(t)] + U [|\psi_l(t)|^2 - 1] \psi_l(t) \quad (2)$$

(with $\psi_0 \equiv \psi_L$) and exhibit the initial and final conditions $|\psi_l(0)|^2 = n_l^{(i)} + 1/2$ and $|\psi_l(T)|^2 = n_l + 1/2$ for all $l = 1, \dots, L$. Each one of those trajectories contributes to the propagator with a complex term whose amplitude is related to the classical stability of the trajectory (i.e., to the Lyapunov exponent in case of chaotic motion) and whose phase is given by the classical action of the trajectory.

Detection probabilities in Fock space are obtained from the square moduli of those matrix elements of the van Vleck–Gutzwiller propagator. The resulting double sum over the above trajectories is substantially simplified upon disorder average, as “off-diagonal” terms in this double sum, involving the contributions of interferences between two different trajectories, exhibit complex phase factors that rapidly vary under a variation of the on-site energies ϵ_l and are therefore averaged to zero as soon as a disorder average is performed. In leading order, we are then left with the *diagonal approximation* which only accounts for pairings of trajectories with themselves in the above double sum. As was elaborated in Ref. [20], the detection probability for the final Fock state $|\mathbf{n}\rangle$ can then be expressed as

$$p_{\mathbf{n}}^{(\text{diag})} = \sum_{\gamma} \left| \det \frac{\partial(\theta_2^{(i)}, \dots, \theta_L^{(i)})_{\gamma}}{\partial(I_2^{(f)}, \dots, I_L^{(f)})} \right|, \quad (3)$$

where we introduce according to $\psi_l(0) \equiv [I_l^{(i)}]^{1/2} \exp[i\theta_l^{(i)}]$ and $\psi_l(T) \equiv [I_l^{(f)}]^{1/2} \exp[i\theta_l^{(f)}]$ the action-angle variables $(I_l^{(i)}, \theta_l^{(i)})$ and $(I_l^{(f)}, \theta_l^{(f)})$ that are associated with the initial and final classical amplitudes on site l , respectively. The Jacobi determinant arising in Eq. (3) excludes one of the sites (which we choose to be site 1 without loss of generality) in order to account for the presence of a cyclic phase that is associated with the total number of particles being a constant of motion [20].

In the presence of fully developed chaos and ergodicity, we can reformulate Eq. (3) as

$$p_{\mathbf{n}}^{(\text{diag})} = \int_0^{2\pi} \frac{d\theta_2}{2\pi} \dots \int_0^{2\pi} \frac{d\theta_L}{2\pi} \prod_{l=2}^L \delta \left[I_l^{(f)} - |\psi_l(T)|^2 \right] \quad (4)$$

using the Hannay–Ozorio de Almeida sum rule [40]. Here $\psi_l(t)$ describes the complex classical amplitude on site l which evolves according to Eq. (2) and emanates from the initial conditions $\psi_l(0) = [n_l^{(i)} + 1/2]^{1/2} \exp[i\theta_l^{(i)}]$ where we set $\theta_1^{(i)} = 0$ without loss of generality. Employing the box regularization $\delta(x) = \theta(d/2 - |x|)/d$ of the delta function with the width $0 < d \ll 1$ (where θ denotes the Heavyside step function), we can numerically

solve Eq. (4) by means of a Monte-Carlo method. $p_{\mathbf{n}}^{(\text{diag})}$ is then obtained in practice by counting the number of Monte-Carlo trajectories that match the required final conditions $|\psi_l(T)|^2 = n_l + 1/2$ for $l = 2, \dots, L$ with the tolerance $\pm d/2$ and by dividing this number by d^{L-1} and by the total number of trial trajectories.

However, care has to be taken as the classical dynamics of the Bose-Hubbard system may not always be fully ergodic. Nonergodicity typically arises if for some disorder realization the on-site energy on one of the sites is substantially higher or lower than the on-site energies of the other sites, in which case this particular site can be considered as being essentially disconnected from the rest of the lattice. The associated angle variable then represents another cyclic variable, which implies that this site has to be excluded in the integrals and the product on the right-hand side of Eq. (4). As a consequence, the associated contribution to $p_{\mathbf{n}}^{(\text{diag})}$ involves a division by d^{L-2} and not d^{L-1} . Evidently, this reasoning straightforwardly generalizes for the case that two or more sites are energetically disconnected from the lattice.

In order to properly account for such nonergodic situations, we numerically determine the effective dimension of the Lagrangian manifold for each trajectory that properly matches the required final conditions. We use the Grassberger-Procaccia algorithm for this purpose [41, 42], i.e., we generate a long time series emanating from the corresponding initial conditions (involving 1000 time steps with the temporal spacing $\Delta t = 0.5\hbar/J$) and determine the correlation dimension of the resulting set of phase-space points. This dimension is then compared with the correlation dimensions that are obtained for a set of randomly chosen phase-space points (ψ_1, \dots, ψ_L) where we impose either no restrictions apart from the conservation of the total number of particles (in which case the resulting set mimicks perfect ergodicity) or additional restrictions concerning the amplitudes on one or several sites. The result of this comparison determines then the power of the tolerance parameter d that we have to use in order to properly count the contribution of the trajectory under consideration.

The resulting classical Fock state probabilities obtained for $d = 0.05$ are displayed as red diamonds in Fig. 2. After the initial transient regime, they agree very well with the quantum probabilities for the states $|\mathbf{n}\rangle \neq |\mathbf{n}^{(i)}\rangle$ that have the same interaction energy as the initial state. The classical diagonal approximation still predicts a slight enhancement of the probability for detecting the initial state $|\mathbf{n}^{(i)}\rangle$ as compared to those other Fock states. This enhancement is, however, much less pronounced than the one that is found for the exact quantum probability $p_{\mathbf{n}^{(i)}}$ (in the absence of time reversal symmetry breaking), the latter being about twice as large as the classical prediction $p_{\mathbf{n}^{(i)}}^{(\text{diag})}$ for long evolution times $T \gg \hbar/J$. This confirms that coherent backscattering, which represents the leading correction to the diagonal approximation [Eq. (3)] for the case $\mathbf{n} = \mathbf{n}^{(i)}$, is at the origin of the enhanced detection probability of the initial

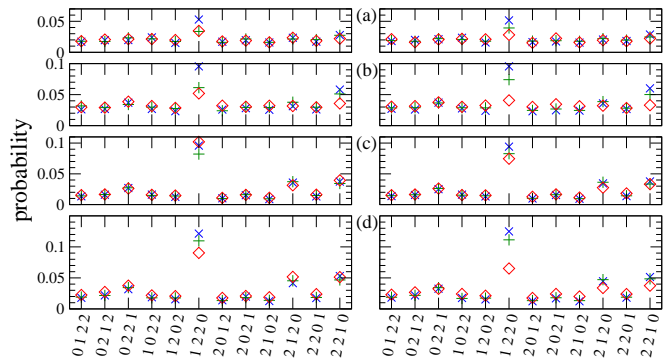


Figure 4: Probabilities for detecting a given Fock state at $JT/\hbar = 10$ (left column) and $JT/\hbar = 100$ (right column) for the lattice parameters (a) $U = J, W = 4J$, (b) $U = 4J, W = 4J$, (c) $U = J, W = 10J$, (d) $U = 4J, W = 10J$. The quantum calculations were done for the initial state $|1, 2, 2, 0\rangle$ and the hopping phases $\varphi = 0$ (blue \times) as well as $\varphi = 0.1\pi$ (green $+$). Red diamonds show the corresponding classical predictions for $\varphi = 0$.

state [43].

V. INTERPLAY WITH MANY-BODY LOCALIZATION

The right column of Fig. 2 shows that the occurrence of coherent backscattering in Fock space has a nonvanishing but quantitatively rather tiny impact on the average populations on the lattice sites, which appears to be too small to be detected in an experiment. In particular, the inhomogeneous distribution of the populations, which reflects the “memory” of the initial state in the time evolution, cannot be entirely traced back to this particular quantum many-body interference phenomenon. Instead, as we can judge from the classical population distributions in the right column of Fig. 2, it seems to dominantly arise from a limitation of the effectiveness of classical ergodicity, due to the fact that for a significant fraction of disorder realizations (and initial on-site angle variables, as discussed in the previous section) the classical energy shell associated with the initial Fock state cannot be efficiently explored and covered within the time scale under consideration. Accordingly, we find in the left column of Fig. 2 that also the classical prediction for the detection probability of the initial state $|1, 2, 2, 0\rangle$ is slightly enhanced with respect to other Fock states on the same energy shell. In contrast to the true quantum detection probability of the initial state, this latter “classical” enhancement appears to decrease with increasing evolution time as we see in Fig. 2(e), in accordance with the expectation that a full classical exploration of the energy shell should, on average, become more and more feasible with increasing evolution time.

As is shown in Fig. 4, this latter tendency to recover classical ergodicity at long evolution times becomes more

pronounced for larger interaction strengths ($U = 4J$), due to the thereby enhanced nonlinear coupling and mixing of single-particle eigenmodes of the disordered system in the discrete Gross-Pitaevskii equation (2). Furthermore, it plays a prominent role in the presence of stronger disorder ($W = 10J$) for which eigenstate thermalization can no longer be taken for granted. In such a situation, we find a highly pronounced enhancement of the detection probability of the initial state which exceeds the probabilities of other states on the same energy shell by about a factor 4 or 5. However, as we can clearly see in the lower two panels on the left column of Fig. 4, this latter enhancement dominantly arises, for finite evolution times $t \sim 10\hbar/J$, due to a deficient ergodicity on the classical level or, more precisely, due to the incapacity of classical trajectories to explore the entire energy shell within those finite time scales. The effectively accessible phase space is therefore rather restricted, which in turn implies, as was pointed out in the supplementary material of Ref. [20], that the set of trajectories that contribute to the backscattering probability mostly contain self-retraced trajectories which are identical to their time-reversed counterparts. The quantum return probability to the initial Fock state is, at $t \sim 10\hbar/J$, therefore only very weakly enhanced (if at all) as compared to its classical prediction, and it is hardly affected by the breaking of time-reversal invariance due to the application of a gauge field.

The right column of Figs. 4(c) and 4(d) confirms that we are concerned here with a typical scenario of many-body localization. While the classical prediction for the detection probability of the initial state decreases at very large evolution times $T \sim 100\hbar/J$, due to the (sub-diffusive) increase of the average classical phase space that can effectively be explored within an increasing evolution time [44–47], the quantum probabilities remain essentially frozen at such large times. We should note that $T = 100\hbar/J$ exceeds the Heisenberg time $\tau \sim \hbar/\Delta$ of the quantum many-body system under consideration, which for $U = J$ and $W = 4J$ exhibits a mean energy spacing of the order of $\Delta \sim 0.05J$ in the central part of its spectrum. This limits the semiclassical relevance of slow classical (sub-)diffusion processes that evolve over such large time scales.

VI. CONCLUSION

In summary, we provided numerical evidence that coherent backscattering in Fock space can arise within

a relatively small many-body system, namely a Bose-Hubbard ring that consists of four sites and contains five particles. The latter can be realized within a single plaquette of a two-dimensional optical square lattice which is to be loaded with five bosonic atoms. The experimental protocol to measure the crucial signature of many-body coherent backscattering, namely the enhancement of the detection probability of the initial state as compared to other Fock states with comparable total energy, involves as major challenges the implementation of state-of-the-art single-site detection techniques [35] as well as a large number of repetitions of the experiment combined with the use of on-site disorder. In addition, a weak artificial gauge field, corresponding to an inter-site hopping that can be as small as $\varphi \simeq \pm 0.02\pi$ (see Fig. 3), ought to be induced within the plaquette in order to break time-reversal invariance and thereby destroy many-body coherent backscattering.

Our study indicates that coherent backscattering in Fock space is most significant and effective in a parameter regime where the many-body system under consideration exhibits eigenstate thermalization. The interplay with many-body localization was briefly discussed but certainly deserves further explorations. In particular, we could speculate that coherent backscattering in Fock space might act as some sort of precursor to many-body localization, in a similar manner as weak localization being a precursor to strong Anderson localization within the single-particle context. More research in this direction, possibly involving a generalization of the self-consistent theory of localization [48] to the many-body domain, appears to be useful in order to clarify this issue and thereby contribute to our understanding of the transition to many-body localization.

Acknowledgments

We thank Thomas Engl, Klaus Richter, Philipp Preiss, and Juan Diego Urbina for useful discussions.

-
- [1] J. M. Deutsch Phys. Rev. A **43**, 2046 (1991).
 - [2] M. Srednicki Phys. Rev. E **50**, 888 (1994).
 - [3] L. D’Alessio, Y. Kafri, A. Polkovnikov, and M. Rigol Adv. Phys. **65**, 239 (2016).
 - [4] M. Rigol, V. Dunjko, and M. Olshanii Nature **452**, 854

- (2008).
- [5] B. L. Altshuler, Y. Gefen, A. Kamenev, and L. S. Levitov Phys. Rev. Lett. **78**, 2803 (1997).
- [6] I. V. Gornyi, A. D. Mirlin, and D. G. Polyakov Phys. Rev. Lett. **95**, 206603 (2005).

- [7] D. M. Basko, I. L. Aleiner, and B. L. Altshuler *Ann. Phys.* **321**, 1126 (2006).
- [8] V. Oganesyan and D. A. Huse *Phys. Rev. B* **75**, 155111 (2007).
- [9] M. Žnidarič, T. Prosen, and P. Prelovšek *Phys. Rev. B* **77**, 064426 (2008).
- [10] J. H. Bardarson, F. Pollmann, and J. E. Moore *Phys. Rev. Lett.* **109**, 017202 (2012).
- [11] M. Serbyn, Z. Papić, and D. A. Abanin *Phys. Rev. Lett.* **111**, 127201 (2013).
- [12] R. Vosk and E. Altman *Phys. Rev. Lett.* **110**, 067204 (2013).
- [13] R. Nandkishore and D. A. Huse *Annu. Rev. Condens. Matter Phys.* **6**, 15 (2015).
- [14] J. Choi, S. Hild, J. Zeiher, P. Schauß, A. Rubio-Abadal, T. Yefsah, V. Khemani, D. A. Huse, I. Bloch, and C. Gross *Science* **352**, 1547 (2016).
- [15] P. W. Anderson *Phys. Rev.* **109**, 1492 (1958).
- [16] M. P. Van Albada and A. Lagendijk *Phys. Rev. Lett.* **55**, 2692 (1985).
- [17] P. E. Wolf and G. Maret *Phys. Rev. Lett.* **55**, 2696 (1985).
- [18] F. Jendrzejewski, K. Müller, J. Richard, A. Date, T. Plisson, P. Bouyer, A. Aspect, and V. Josse *Phys. Rev. Lett.* **109**, 195302 (2012).
- [19] K. Richter and M. Sieber *Phys. Rev. Lett.* **89**, 206801 (2002).
- [20] T. Engl, J. Dujardin, A. Argüelles, P. Schlagheck, K. Richter, and J. D. Urbina *Phys. Rev. Lett.* **112**, 140403 (2014).
- [21] T. Engl, J. D. Urbina, and K. Richter *Phil. Trans. R. Soc. A* **374**, 20150159 (2016).
- [22] T. Engl, P. Plöb, J. D. Urbina, and K. Richter *Theor. Chem. Acc.* **133**, 1563 (2014).
- [23] T. Engl, J. D. Urbina, K. Richter, and P. Schlagheck [arXiv:1409.5684](https://arxiv.org/abs/1409.5684) (2014).
- [24] S. Fölling, S. Trotzky, P. Cheinet, M. Feld, R. Saers, A. Widera, T. Müller, and I. Bloch *Nature* **448**, 1029 (2007).
- [25] P. Cheinet, S. Trotzky, M. Feld, U. Schnorrberger, M. Moreno-Cardoner, S. Fölling, and I. Bloch *Phys. Rev. Lett.* **101**, 090404 (2008).
- [26] Y. J. Lin, R. L. Compton, K. Jiménez-García, J. V. Porto, and I. B. Spielman *Nature* **462**, 628 (2009).
- [27] N. Goldman, I. Satija, P. Nikolic, A. Bermudez, M. A. Martin-Delgado, M. Lewenstein, and I. B. Spielman *Phys. Rev. Lett.* **105**, 255302 (2010).
- [28] J. Dalibard, F. Gerbier, G. Juzeliūnas, and P. Öhberg *Rev. Mod. Phys.* **83**, 1523 (2011).
- [29] Detections of the atomic populations on the lattice sites can be carried out right after this preparation process to verify its reliability in practice.
- [30] J. E. Lye, L. Fallani, M. Modugno, D. S. Wiersma, C. Fort, and M. Inguscio *Phys. Rev. Lett.* **95**, 070401 (2005).
- [31] J. Billy, V. Josse, Z. Zuo, A. Bernard, B. Hambrecht, P. Lugan, D. Clément, L. Sanchez-Palencia, P. Bouyer, and A. Aspect *Nature* **453**(June), 891 (2008).
- [32] We thereby neglect spatial correlations that would necessarily arise within disordered potentials realized by speckle fields.
- [33] W. S. Bakr, J. I. Gillen, A. Peng, S. Fölling, and M. Greiner *Nature* **462**, 74 (2009).
- [34] J. F. Sherson, C. Weitenberg, M. Endres, M. Cheneau, I. Bloch, and S. Kuhr *Nature* **467**, 68 (2010).
- [35] A. M. Kaufman, M. E. Tai, A. Lukin, M. Rispoli, R. Schittko, P. M. Preiss, and M. Greiner *Science* **353**, 794 (2016).
- [36] We do not account for three-body losses that could arise if three atoms are located on the same site.
- [37] E. Akkermans and G. Montambaux, *Mesoscopic Physics of Electrons and Photons* (Cambridge University Press, Cambridge, 2007).
- [38] G. Labeyrie, T. Karpiuk, J. F. Schaff, B. Grémaud, C. Miniatura, and D. Delande *EPL* **100**, 66001 (2012).
- [39] M. C. Gutzwiller, *Chaos in Classical and Quantum Mechanics* (Springer, New York, 1990).
- [40] J. H. Hannay and A. M. Ozorio De Almeida *J. Phys. A: Math. Gen.* **17**, 3429 (1984).
- [41] P. Grassberger and I. Procaccia *Phys. Rev. Lett.* **50**, 346 (1983).
- [42] P. Grassberger and I. Procaccia *Physica D* **9**, 189 (1983).
- [43] For short evolution times, a macroscopic fraction of backscattered trajectories are self-retraced, meaning that they are identical with their time-reversed counterpart, as was argued in the supplementary material of Ref. [20]. This gives rise to a weaker enhancement of the quantum probability for detecting the initial state with respect to the classical prediction.
- [44] D. L. Shepelyansky *Phys. Rev. Lett.* **70**, 1787 (1993).
- [45] A. S. Pikovsky and D. L. Shepelyansky *Phys. Rev. Lett.* **100**, 094101 (2008).
- [46] S. Flach, D. O. Krimer, and C. Skokos *Phys. Rev. Lett.* **102**, 024101 (2009).
- [47] G. Kopidakis, S. Komineas, S. Flach, and S. Aubry *Phys. Rev. Lett.* **100**, 084103 (2008).
- [48] D. Vollhardt and P. Wölfle *Phys. Rev. Lett.* **48**, 699 (1982).